OBSERVATIONS OF THERMAL TIDES IN THE MIDDLE ATMOSPHERE OF MARS BY THE SPICAM INSTRUMENT.

P. Withers, R. D. Pratt, *Boston University, Boston, USA (withers@bu.edu)***, J.-L. Bertaux, F. Montmessin,** *Service d'Aéronomie du CNRS, Verrières-le-Buisson, France.***, J. F. Forbes, Y. Moudden,** *University of Colorado, Boulder, USA.*

Introduction

Global-scale oscillations in atmospheric state variables, such as density, pressure and temperature, that are driven by periodic solar forcing are known as thermal tides (*Chapman and Lindzen*, 1970; *Forbes*, 1995). Thermal tides are particularly prominent on Mars due to its rapid rotation rate and the low atmospheric density at its surface (*Zurek*, 1976; *Wilson and Hamilton*, 1996; *Zurek et al.*, 1992). The most well-studied martian tidal modes are migrating tidal modes, which have the same phase speed as the Sun, and three non-migrating tidal modes, which do not. These have the following periods and zonal wavenumbers: $n = 1, s = -1$, $n = 1, s = -2$ and $n = 2, s = -1$, where n=1 is a diurnal period and n=2 is a semi-diurnal period. The dominant Hough modes for these three non-migrating tidal modes, respectively, are the diurnal Kelvin wave known as DK1, the diurnal Kelvin wave known as DK2, and the semi-diurnal Kelvin wave known as SK1 (*Chapman and Lindzen*, 1970; *Andrews et al.*, 1987; *Forbes*, 1995). In a fi ed local time reference frame, DK1 causes wave-2 zonal variations and DK2 and SK1 cause wave-3 zonal variations. All three of these have been observed throughout the martian atmosphere.

The objectives of this work are to use observations from the SPICAM UV spectrometer instrument on Mars Express (MEX) (*Bertaux et al.*, 2004; *Quémerais et al.*, 2006) to characterize the predominant tidal components in the middle atmosphere and to relate tides in the middle atmosphere to tides at other altitudes. We use individual stellar occultation profile of atmospheric density, pressure and temperature to construct two dimensional slices of pressure and temperature as functions of longitude and altitude at fi ed season, latitude and local time. Tides can cause these atmospheric state variables to vary with longitude and for the amplitudes and phases of these zonal variations to depend on altitude.

SPICAM profiles

Recent measurements of hundreds of vertical profile of atmospheric density, pressure and temperature between $\sim$20 km and $\sim$120 km by the SPICAM instrument on ESA's MEX spacecraft are well-suited for studies of thermal tides in the middle atmosphere (*Bertaux et al.*, 2004; *Quémerais et al.*, 2006). SPICAM is a UV spectrometer that can record a star's spectrum during a stellar occultation (*Bertaux et al.*, 2004). Attenuation of starlight along the ray path is controlled by the altitude-dependent slant column density of atmospheric constituents and the wavelength-dependent absorption cross-sections of these constituents. A vertical profil of CO_2 number density has been determined from each stellar occultation observed by SPICAM and vertical profile of mass density, pressure and temperature have been determined from each profil of CO_2 number density (*Quémerais et al.*, 2006). Although formal results have been obtained down to $\sim$20 km, the effects of dust make the derived atmospheric properties unreliable below 50 km (*Quémerais et al.*, 2006; *Forget et al.*, 2009). *Forget et al.* (2009) and *McDunn et al.* (2010) have analysed the SPICAM profile to study the thermal structure and dynamics of the middle atmosphere of Mars, as well as the processes that control them.

We have identifie four Cases in which multiple SPICAM profile were obtained within narrow ranges of Ls, LST and latitude, yet sampled all longitudes (Table 1). Thermal tides, if present, will produce zonal variations in each of these Cases.

Analysis

Figure 1 uses data at 110 km altitude from Case C to illustrate that substantial variations in pressure with longitude at fi ed altitude are apparent in SPICAM observations. These variations are caused by non-migrating thermal tides. Figure 1 also displays a harmonic fi to the data. The wave-2 component is strongest and the wave-3 component is also significant but the wave-1 component is weak, which is consistent with previous work at thermospheric altitudes and theoretical predictions concerning the importance of DK1, DK2 and SK1. However, Figure 2 shows that the amplitude of the wave-2 component is unusually small, 0.013 ± 0.047 at 110 km, in Case D. This component's fitte amplitude exceeds 0.2 at 110 km in Cases A—C and is also large in most MGS accelerometer density observations at 130 km (*Withers et al.*, 2003). The unprecedented weakness of the wave-2 component extends over all altitudes in this Case and is a major puzzle.

Figures 3-4 report the amplitudes and phases of harmonic components in Case C as a function of altitude. The steep increase in wave-2 amplitude above 90 km is consistent with weak dissipation, which is a characteristic of the DK1 tidal mode (*Forbes and Hagan*, 2000).

Table 1: Cases where multiple SPICAM profile were obtained within narrow range of Ls, LST and latitude. N is the number of profile in each Case.

Case	N	Latitude	Ls	LST (hrs)
A	53	60°S–30°S	90°–120°	1.0–5.0
B	29	15°N–45°N	240°–270°	0.8–3.5
C	34	20°S–10°S	90°–120°	2.6–4.8
D	27	40°S–30°S	150°–180°	22–24

However, this poses the question of why the amplitude of the wave-2 component is appreciable, rather than negligibly small, below 90 km. The likely explanation is that the amplitude of the DK1 tidal mode is extremely small at lower altitudes, but that some other tidal mode that is more sensitive to dissipative processes is responsible for the observed wave-2 component at lower altitudes. This also provides a natural explanation for 20° eastward shift in the wave-2 phase around 90 km.

Zonal variations in temperature can also be explored (Figures 5-7). From theoretical considerations of a single tidal mode, the minimum in the wave-2 component of pressure amplitude at 90 km should be accompanied by a reversal (change by 90 degrees or half of its full range) in the corresponding temperature phase, but this is not observed. The implication is that multiple tidal modes contribute to the wave-2 variations in pressure at this altitude.

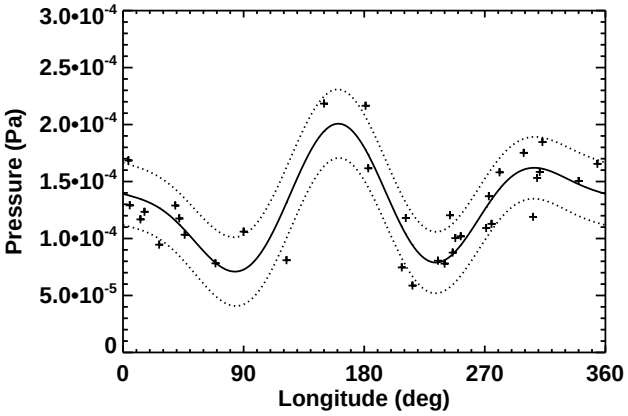

Figure 1: Crosses show pressure measurements at 110 km for Case C. The solid line is a harmonic fi (up to wavenumber 3) to the data and the two dotted lines indicate the 1σ uncertainty envelope about the fit

Summary

Wave-2 zonal variations in atmospheric state variables in the middle atmosphere of Mars for Case C are dominated by the well-known DK1 tidal mode above 90 km, but by multiple tidal modes at lower altitudes. Similar analysis can be applied to other harmonic components and other Cases to explore the dominant tidal modes in the middle atmosphere of Mars. The behaviour of the wave-3 component in several Cases is consistent with dominance by a single tidal mode, but phase changes with local time suggest that the dominant mode is DK2 in the tropics and SK1 at more poleward latitudes.

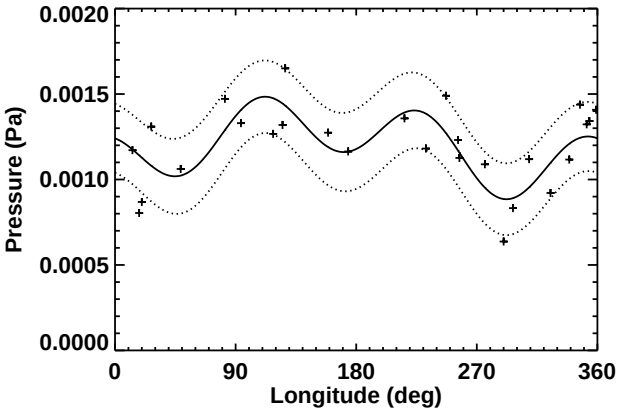

Figure 2: As Figure 1, but for Case D.

References

Andrews, D. G., J. R. Holton, and C. B. Leovy (1987), *Middle atmosphere dynamics*, Academic Press, San Diego.

Bertaux, J.-L., D. Fonteyn, O. Korablev, E. Chassefre, E. Dimarellis, J. P. Dubois, A. Hauchecorne, F. Lefèvre, M. Cabane, P. Rannou, A. C. Levasseur-Regourd, G. Cernogora, E. Quemerais, C. Hermans, G. Kockarts, C. Lippens, M. de Maziere, D. Moreau,

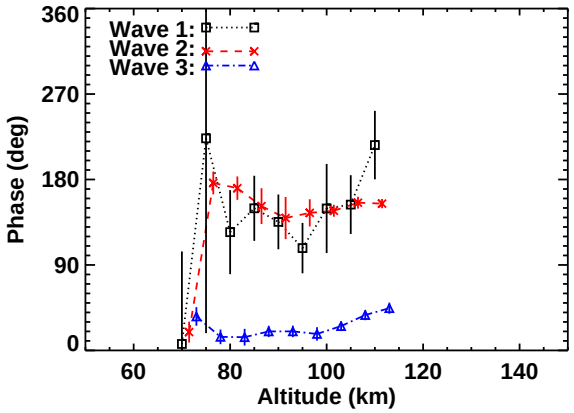

Figure 3: Fitted phases and 1σ uncertainties for pressure measurements at 5 km intervals for Case C. Black squares identify wave-1, red crosses identify wave-2, and blue triangles identify wave-3. To minimize confusion caused by overlapping symbols, wave-2 and wave-3 symbols are plotted slightly above their actual altitudes.

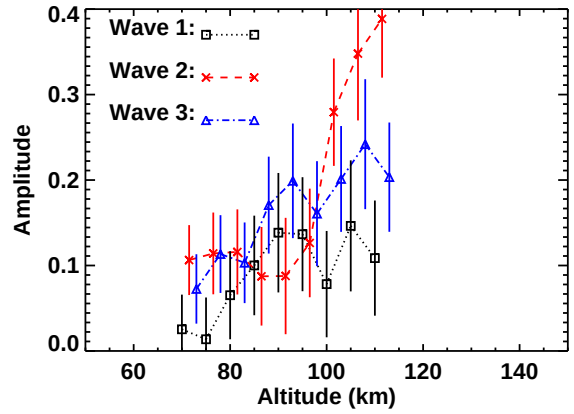

Figure 4: Fitted normalized amplitudes and 1σ uncertainties for pressure measurements at 5 km intervals for Case C. Symbols and vertical offsets are same as in Figure 3.

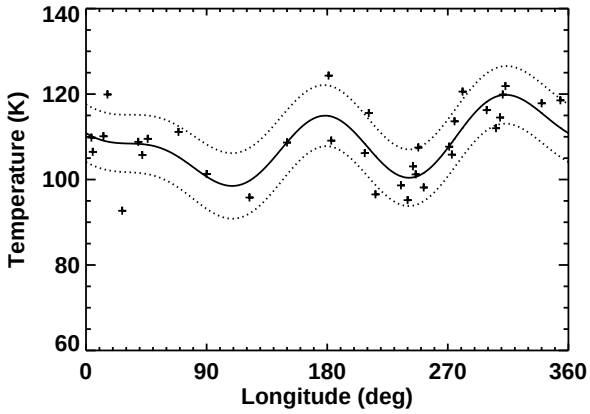

Figure 5: As Figure 1, but for temperature at 100 km in Case C. Pressure and temperature phases are anti-correlated (differ by 90 degrees or half of the full range) for the wave-1 component and correlated (similar) for the wave-2 component.

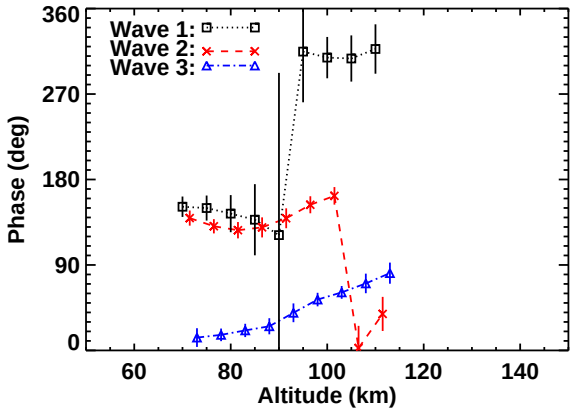

Figure 6: As Figure 3, but for temperature.

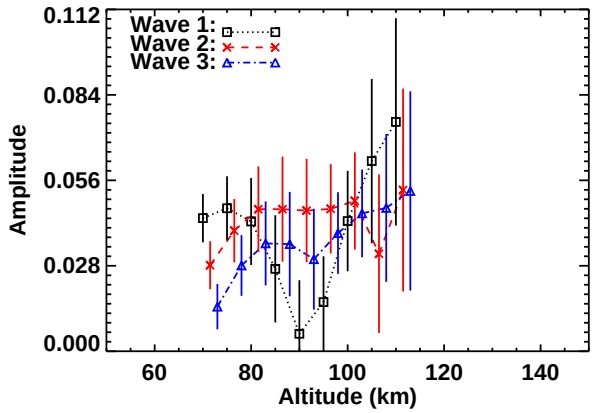

Figure 7: As Figure 4, but for temperature.

C. Muller, E. Neefs, P. C. Simon, F. Forget, F. Hourdin, O. Talagrand, V. I. Moroz, A. Rodin, B. Sandel, and A. Stern (2004), *SPICAM: Studying the global structure and composition of the Martian atmosphere*, pp. 95–120, ESA SP-1240: Mars Express: the Scientifi Payload, available online at http://sci.esa.int/science-e/www/object/index.cfm?fobjectid=34885.

Chapman, S., and R. Lindzen (1970), *Atmospheric tides. Thermal and gravitational*, Reidel, Dordrecht, Germany.

Forbes, J. F. (1995), Tidal and planetary waves, in *The upper mesosphere and lower thermosphere: A review of experiment and theory*, edited by R. M. Johnson and T. L. Killeen, pp. 67–87, American Geophysical Union, Washington, DC.

Forbes, J. M., and M. E. Hagan (2000), Diurnal Kelvin wave in the atmosphere of Mars: Towards an understanding of "stationary" density structures observed by the MGS Accelerometer, *Geophys. Res. Lett.*, *27*, 3563–3566.

Forget, F., F. Montmessin, J. Bertaux, F. González-Galindo, S. Lebonnois, E. Quémerais, A. Reberac, E. Dimarellis, and M. A. López-Valverde (2009), Density and temperatures of the upper Martian atmosphere measured by stellar occultations with Mars Express SPICAM, *J. Geophys. Res.*, *114*, E01004, doi: 10.1029/2008JE003086.

McDunn, T. L., S. W. Bougher, J. Murphy, M. D. Smith, F. Forget, J. Bertaux, and F. Montmessin (2010), Simulating the density and thermal structure of the middle atmosphere (80-130 km) of Mars using the MGCM-MTGCM: A comparison with MEX/SPICAM observations, *Icarus*, *206*, 5–17, doi: 10.1016/j.icarus.2009.06.034.

Quémerais, E., J.-L. Bertaux, O. Korablev, E. Dimarellis, C. Cot, B. R. Sandel, and D. Fussen (2006), Stellar occultations observed by SPICAM on Mars Express, *J. Geophys. Res.*, *111*, E09S04, doi: 10.1029/2005JE002604.

Wilson, R. J., and K. Hamilton (1996), Comprehensive model simulation of thermal tides in the Martian atmosphere, *J. Atmos. Sci.*, *43*, 1290–1326.

Withers, P., S. W. Bougher, and G. M. Keating (2003), The effects of topographically-controlled thermal tides in the martian upper atmosphere as seen by the MGS accelerometer, *Icarus*, *164*, 14–32.

Zurek, R. W. (1976), Diurnal tide in the martian atmosphere, *J. Atmos. Sci.*, *33*, 321–337.

Zurek, R. W., J. R. Barnes, R. M. Haberle, J. B. Pollack, J. E. Tillman, and C. B. Leovy (1992), Dynamics of the atmosphere of Mars, in *Mars*, edited by H. H. Kieffer, B. M. Jakosky, C. W. Snyder, and M. S. Matthews, pp. 835–933, University of Arizona Press.